Catalysis Today 176 (2011) 139–143

Contents lists available at ScienceDirect

Catalysis Today

journal homepage: www.elsevier.com/locate/cattod

CO_2 reforming of CH_4 over Co–Mg–Al mixed oxides prepared via hydrotalcite like precursors

Cédric Gennequin*, Maryam Safariamin, Stéphane Siffert, Antoine Aboukaïs, Edmond Abi-Aad

Université Lille Nord de France, F-59000 Lille, FranceUnité de chimie environnementale et interactions sur le vivant EA 4492, Université du Littoral Côte d'Opale, 145 avenue Maurice Schumann, 59140 Dunkerque, France

ARTICLE INFO

Article history:
Received 30 September 2010
Received in revised form
23 December 2010
Accepted 24 January 2011
Available online 22 February 2011

Keywords:
Hydrotalcite
Dry reforming of methane
Cobalt
Carbon formation

ABSTRACT

$Co_xMg_{6-x}Al_2$ (with $x = 0$, 2, 4, and 6) mixed oxides catalysts were synthesized via hydrotalcite precursors. The catalytic performance and stability were studied in dry reforming of methane. Regardless of the amount of coke deposited on the Co_6Al_2HT500 catalyst, no loss of activity was observed during 24 h on stream indicating that part of this carbon is not poisonous. $Co_4Mg_2Al_2$HT500 was undergoing a severe deactivation after 11 h on stream. The XRD result revealed an important sintering phenomenon of metal particles. $Co_2Mg_4Al_2$HT500 has shown a stable performance for 24 h on stream without any deactivation or coke deposition, displaying very good stability. This performance was explained by the stability of crystallite size of metal particles and by the presence of $MgAl_2O_4$ phase known for its basic properties.

1. Introduction

CO_2 reforming of methane ($CH_4 + CO_2 \rightarrow 2CO + 2H_2$ ($\Delta H_{298}{}^\circ = 247$ kJ/mol)) presents a double interest due to the production of syngas and the fact of consuming carbon dioxide; this latter is an important agent of the greenhouse effect. Dry reforming of methane is generally performed with catalysts based on noble metals [1] or transition metals as nickel or cobalt [2–4]. The major problem of this reaction is the deactivation by carbon deposition [5]. To minimize this problem, several authors suggest the use of supports possessing basic characters, and/or allowing to better dispersion of the active phase [6,7]. The objective of this work is the catalytic study of mixed oxides issued of Co/Mg/Al hydrotalcites (LDH) with different molar ratio as precursors for the dry reforming of methane. Cobalt is known as an active metal for this reaction [3] and mixed oxides obtained from hydrotalcites-like compounds exhibit basic properties as well as higher dispersion of the active phase [8]. Moreover catalyst surface basicity helps to suppress carbon deposition by promoting the activation of CO_2 on the surface of catalysts. Indeed, an interesting way to obtain mixed oxides catalysts is through the use of hydrotalcites as precursors.

2. Experimental

Four samples with different Co and Mg contents were synthesized using hydrotalcite method [9]: $Co_xMg_{6-x}Al_2$HT with $x = 0$, 2, 4, and 6. The calcination treatment of solids was performed under a flow of air (4 L h^{-1}/2 °C min^{-1} 4 h at 500 °C). Differential thermal and thermogravimetric analyses (DTA/TG) (Netzsch STA 409 equipped with a microbalance) were conducted in air at a heating rate of 5 °C min^{-1} (25–1000 °C). The structure of solids was analyzed at room temperature by X-ray diffraction (XRD) technique using a Bruker D8 Advance diffractometer equipped with a copper anode ($\lambda = 1.5406$ Å). Diffraction patterns were recorded over a 2Θ range of 4–80° and using a step size of 0.02 and a step time of 6 s. The mean crystallite sizes were estimated using the Scherrer equation. Catalytic tests were performed under atmospheric pressure. 100 mg of powder samples are placed in fixed bed quartz reactor. The reactants and products are analyzed with an on-line in a Varian 3600 chromatograph equipped with a CTRI column and a thermal conductivity detector. Before testing, calcined catalysts were treated with pure nitrogen (25–400 °C; 10 °C min^{-1}), after the sample is reduced or not with pure hydrogen flow (25–800 °C; 10 °C min^{-1}). Then the reactor is fed with the reagent gas mixture diluted with Ar ($CH_4/CO_2 = 1$), with a total flow rate of 100 mL min^{-1}.

The determination of methane and carbon dioxide conversions were calculated as follows:

$$X_{CH_4\,\text{conversion}}\ (\%) = \frac{(CH_4)_{in} - (CH_4)_{out}}{(CH_4)_{in}} \times 100$$

* Corresponding author at: Unité de chimie environnementale et interactions sur le vivant EA 4492, Université du Littoral Côte d'Opale, 145 avenue Maurice Schumann, 59140 Dunkerque, France. Tel.: +33 3 28 65 82 61.
E-mail address: cedric.gennequin@univ-littoral.fr (C. Gennequin).

0920-5861/$ – see front matter © 2011 Elsevier B.V. All rights reserved.
doi:10.1016/j.cattod.2011.01.029

Table 1
XCH_4/XCO_2, CO_2/CO, H_2/CH_4 ratio versus temperature and theoretical equilibrium CH_4 and CO_2 conversions.

T (°C)	XCH_4/XCO_2	CO_2/CO	H_2/CH_4
Co_6Al_2HT500			
450	0.94	0.58	1.13
550	1.43	0.62	1.40
650	1.11	0.53	1.57
750	1.01	0.51	1.62
$Co_4Mg_2Al_2$HT500			
450	0.16	0.86	1.86
550	0.86	0.54	1.48
650	1.05	0.51	1.54
750	1.08	0.48	1.49
$Co_2Mg_4Al_2$HT500			
450	0.63	0.62	1.31
550	0.84	0.55	1.46
650	0.94	0.53	1.55
750	0.99	0.50	1.61
Thermodynamic equilibrium (at 700 °C)		XCO_2 or XCH_4	72.3%

$$XCO_{2\,\text{conversion}}\ (\%) = \frac{(CO_2)_{in} - (CO_2)_{out}}{(CO_2)_{in}} \times 100$$

The different ratio is presented in Table 1 and carbon balances were calculated as follows:

$$H_2/CO\ \text{ratio}\ \ (\text{for example}) = \frac{\text{moles of } H_2 \text{ produced}}{\text{moles of CO produced}}$$

$$\text{Carbon balance} = \frac{(CH_4)_{out} + (CO_2)_{out} + (CO)_{out}}{(CH_4)_{in} + (CO_2)_{in}} \times 100$$

The product selectivity is represented as the molar ratio of H_2/CO. The comparisons of the activities of these catalysts were primarily characterized by the conversion and the product selectivity criteria.

3. Results and discussion

3.1. Catalysts characterization

A detailed characterization of these catalysts can be found elsewhere [9]. In summary, the calcination at 500 °C of "HT" samples leads to a mixture of three oxide spinel phases: Co_3O_4, $CoAl_2O_4$ and Co_2AlO_4. Fig. 1a presents the XRD patterns of the reduced samples before test. For all samples Co^0 is observed. For $Co_2Mg_4Al_2$HT500 and $Co_4Mg_2Al_2$HT500, the presence of spinel phase such as $MgAl_2O_4$ and $CoAl_2O_4$ is observed. For Co_6Al_2HT500, the peaks corresponding to the $CoAl_2O_4$ spinel structure are observed. The partial Co^0 oxidation into $CoAl_2O_4$ spinel takes place during the XRD analysis. This result indicates the stability of this structure under air at ambient temperature.

3.2. Catalytic activity

Solids did not show significant activity without reduction pretreatment (Fig. 2a). The low reforming activity can be assigned to the absence of metallic phase which is necessary to the adsorption and the activation of the reactants [4]. In the case of $Co_xMg_{6-x}Al_2$HT catalysts, reduction pre-treatment at 800 °C (1 h under pure H_2 flow 40 mL min^{-1}) strongly influenced the activity and selectivity. Fig. 2a–d illustrates the evolution of methane and CO_2 conversions obtained, at various temperatures, for reduced catalysts. The initial activity by comparison of methane conversion (Fig. 2a) follows the order: Co_6Al_2HT500 > $Co_4Mg_2Al_2$HT500 > $Co_2Mg_4Al_2$HT500 > Mg_6Al_2HT500.

The calculation of the equilibrium conversion for CO_2 reforming of methane at 700 °C for a CH_4/CO_2 feed ratio of 1/1 at atmospheric pressure is added in Table 1. This calculation is based on the assumption that only reforming reaction occurs without any side reactions. As the equivalent reaction stoichiometric, the CH_4 and CO_2 conversions should be equal and the H_2/CO ratio should be unity at all temperatures. However, the results obtained on CO_2 reforming of methane have discrepancies with the equilibrium results. The CO_2 conversion is different from that of CH_4 and the H_2/CO ratio is below unity (Table 1 and Figs. 2 and 3c). These results reveal that unfavourable reactions have strong influence on the performance of the reforming reaction and contribute to the reactants consumption without being strictly accounted for in equilibrium calculation as shown the studies of Haag et al. [10] and Avila-Neto et al. [11]. Their data show that the experimental result appears above the equilibrium curves, suggesting the formation of coke on the surface of the catalysts [11].

As illustrated in Fig. 3a, an amount of water is formed at the temperature range from 450 to 700 °C and reached a maximum at 550–600 °C beyond which the water yield decreased and the water formation is suppressed at higher temperatures. In parallel, at the same temperature range, an amount of carbon is formed as shown in Fig. 3b by an important negative carbon estimation. This result can be attributed to two reactions: the reverse water–gas shift reaction ($CO_2 + H_2 \rightarrow CO + H_2O$ (ΔH_{298} ° = 41 kJ/mol)) which led to the formation of CO and water and the reverse carbon gasification reaction ($CO + H_2 \rightarrow C + H_2O$ (ΔH_{298} ° = – 131 kJ/mol)) which led to the formation of carbon and water (Fig. 3a and b). During, the reverse water-gas shift reaction, CO_2 react with H_2 to produce CO and water in accordance with the experimental ratio presented in Table 1 (the ratio are lower than those provided by the dry reforming reaction only, for example H_2 is consumed and CO is produced which leads to

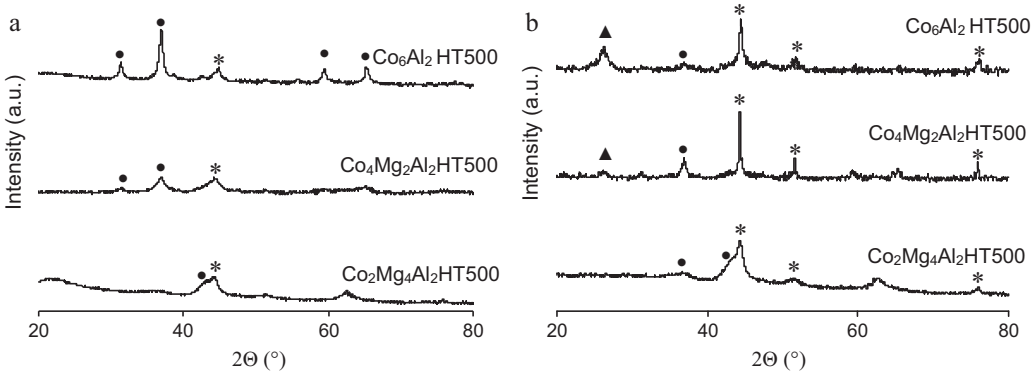

Fig. 1. XRD patterns of $Co_xMg_yAl_2$HT500 after H_2 reduction (a) and after catalytic test (b). *: Co^0: JCPDS 150806; ●: spinel ($CoAl_2O_4$: JCPDS: 822239; $MgAl_2O_4$: JCPDS: 211152) ▲: graphite carbon: JCPDS 751621.

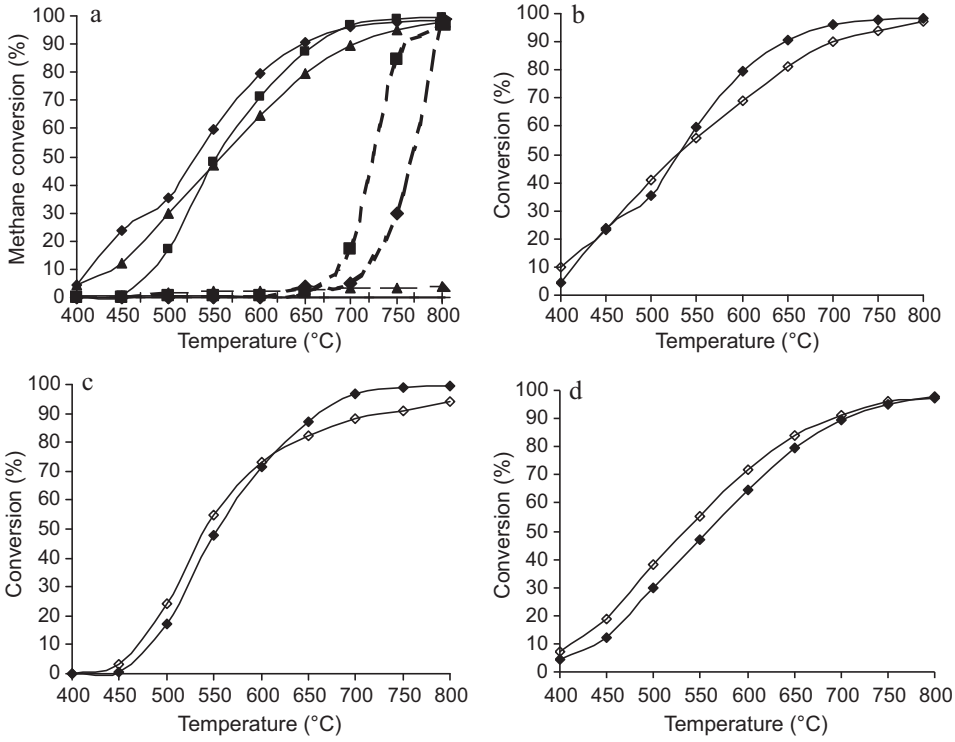

Fig. 2. Comparison of methane conversion over $Co_xMg_yAl_2HT500$ non reduced samples (--) and $Co_xMg_yAl_2HT500$ reduced samples (—) (a) (♦: Co_6Al_2HT500; ■: $Co_4Mg_2Al_2HT500$; ▲: $Co_2Mg_4Al_2HT500$; +: Mg_6Al_2HT500). Methane and CO_2 conversions of Co_6Al_2HT500 reduced sample (b); $Co_4Mg_2Al_2HT500$ reduced sample (c) and $Co_2Mg_4Al_2HT500$ reduced sample (d) (♦: CH_4 conversion; ◊: CO_2 conversion).

a H_2/CO ratio below 1; CO_2 is consumed which leads to XCH_4/XCO_2 ratio below 1).

Fig. 3a indicates, for temperatures higher than 550–600 °C, the drastic reduction of water formation. Steam reforming of methane reaction ($CH_4 + H_2O \rightarrow 3H_2 + CO$ ($\Delta H_{298}{}^\circ = 206$ kJ/mol)) has also to be considered.

For $Co_4Mg_2Al_2HT500$ and Co_6Al_2HT500, the contribution of the steam reforming reaction is visible at 550 °C and 600 °C, respectively, in accordance with the results presented in Table 1 and Fig. 2b and c. Indeed, at these temperatures, the CH_4 conversion is higher than that of CO_2 which is ascribed to the CH_4 consumption by the steam reforming reaction. Moreover, the H_2/CO ratio reached maximum which is ascribed to the H_2 formation by the steam reforming reaction.

The methane cracking reaction ($CH_4 \rightarrow C + 2H_2$ ($\Delta H_{298}{}^\circ = 206$ kJ/mol)) may also occur leading to the production of carbon (deficiency of carbon balance, consumption of CH_4 and H_2 production).

The catalytic behaviour of $Co_2Mg_4Al_2HT500$ solid is different compared to the other catalysts. Water production is lower than for other catalysts and methane conversion is always lower than that of CO_2. Indeed, the CO_2 conversion higher than the CH_4 conversion (Fig. 2c and Table 1) can have several origins: a trapping effect of CO_2 by the basic sites of the surface (described in the following section) may contribute to displace the equilibrium towards higher conversion. Such an effect would only be transient till the adsorption capacity of the surface is reached. Another reactions can explain the results, the reverse of Boudouard reaction $C + CO_2 \rightarrow 2CO$ also contribute to the CO_2 and carbon consumptions and may explain the observed carbon balance (Fig. 3a), the XCH_4/XCO_2 ratio in Table 1 and the H_2/CO ratio. The carbon produced can be also consumed by the reaction $C + H_2O \rightarrow CO + H_2$ (water is consumed and may explain the low amount of water observed Fig. 3a). H_2 and CO are produced and can explain the H_2/CO ratio presented in Fig. 3c.

3.3. Catalysts stability

The activity and stability of the prepared catalysts are examined for a period of about 24 h on stream at 700 °C (Fig. 4). Co_6Al_2HT500 and $Co_2Mg_4Al_2HT500$ are stable with time under flow. $Co_4Mg_2Al_2HT500$ shows a higher deactivation after about 11 h on stream. One possible reason for such deactivation could be the loss of active phase area due to severe sintering of metal particles or by blocking of the metal surface sites by carbonaceous deposits or oxidation of the metal. Different types of coke deposits have been reported for methane reforming on catalysts, such as adsorbed atomic carbon, amorphous carbon, bulk carbide, and crystalline graphitic carbon. After experiment, Co_6Al_2HT500; $Co_4Mg_2Al_2HT500$ and $Co_2Mg_4Al_2HT500$ are characterized by TG–DTA (Fig. 5a–c). Catalysts exhibit a weight decrease corresponding to carbon oxidation, the following order is obtained for carbon amount: Co_6Al_2HT500 (−52%) > $Co_4Mg_2Al_2HT500$ (−23%) > $Co_2Mg_4Al_2HT500$ (−5.5%).

For Co_6Al_2HT500 and $Co_4Mg_2Al_2HT500$, the oxidation of coke occurred mainly at 400–550 °C in accordance with the DTA and DTG curves. For $Co_2Mg_4Al_2HT500$, no considerable exothermic phenomenon is observed (Fig. 5c) in a temperature range of 190–900 °C.

Thus, Co_6Al_2HT500 and $Co_4Mg_2Al_2HT500$ show a strong total amount of deposited carbon and the weight loss observed can be ascribed to coke containing hydrogen (CH_x) and or surface carbon [4,12]. For these catalysts containing a considerable amount of deposited carbon, crystalline plane of graphite like structures is also visible (Fig. 1b) by the graphite carbon peak which appears at $2\Theta = 26.3°$. Regardless of the amount of coke deposited on the Co_6Al_2HT500 catalyst, no loss of activity is observed during 24 h on stream indicating that part of this carbon is not poisonous. But $Co_4Mg_2Al_2HT500$ undergoes severe deactivation after 11 h on stream. In our case, the catalyst activity has not been influenced by the carbon deposition after 24 h. This behaviour could be related to the carbon deposition sites

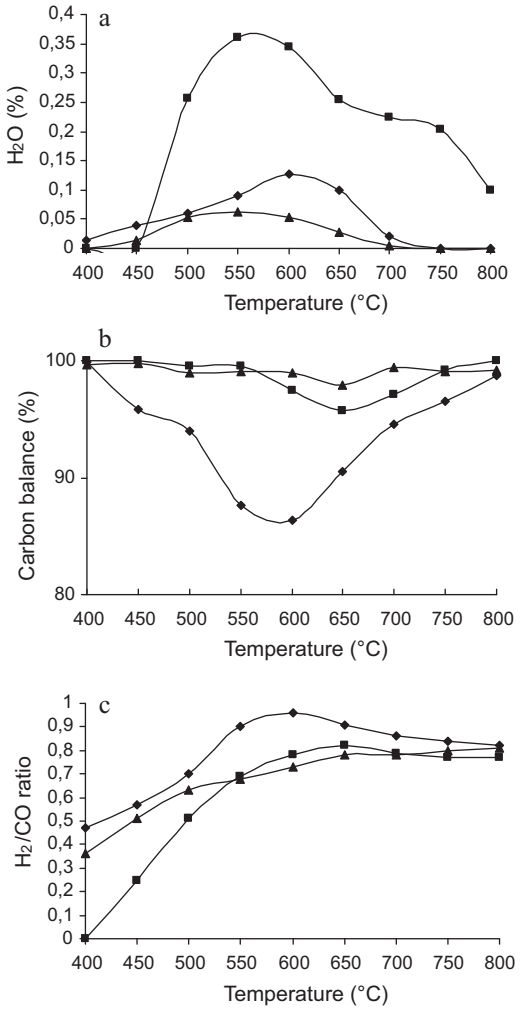

Fig. 3. Water formation versus temperature (a); carbon balance versus temperature (b); H_2/CO ratio versus temperature (c) (♦: Co_6Al_2HT500; ■: $Co_4Mg_2Al_2HT500$; ▲: $Co_2Mg_4Al_2HT500$).

and/or the ability of carbon to play a role as a reaction intermediate. In accordance with the literature data, graphite (detected by XRD, Fig. 1b) can favour close contact of coke and metal, acts as CH_x collector and reduces the time of carbon species residence on the metal surface, what can limit deactivation process of catalyst surface despite the large amount of carbon deposit [13–16]. The presence of carbon species deposited on the surface

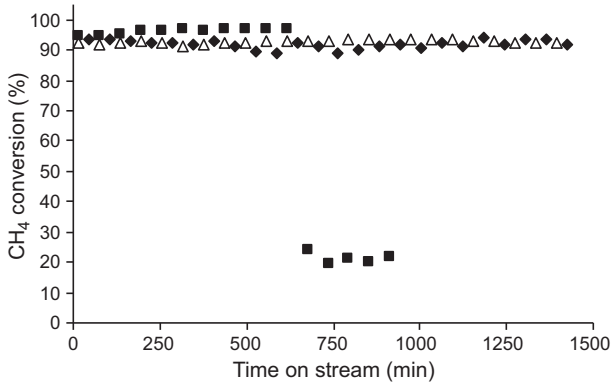

Fig. 4. Stability test for $Co_xMg_yAl_2HT500$ reduced samples (♦: Co_6Al_2HT500; ■: $Co_4Mg_2Al_2HT500$; △: $Co_2Mg_4Al_2HT500$).

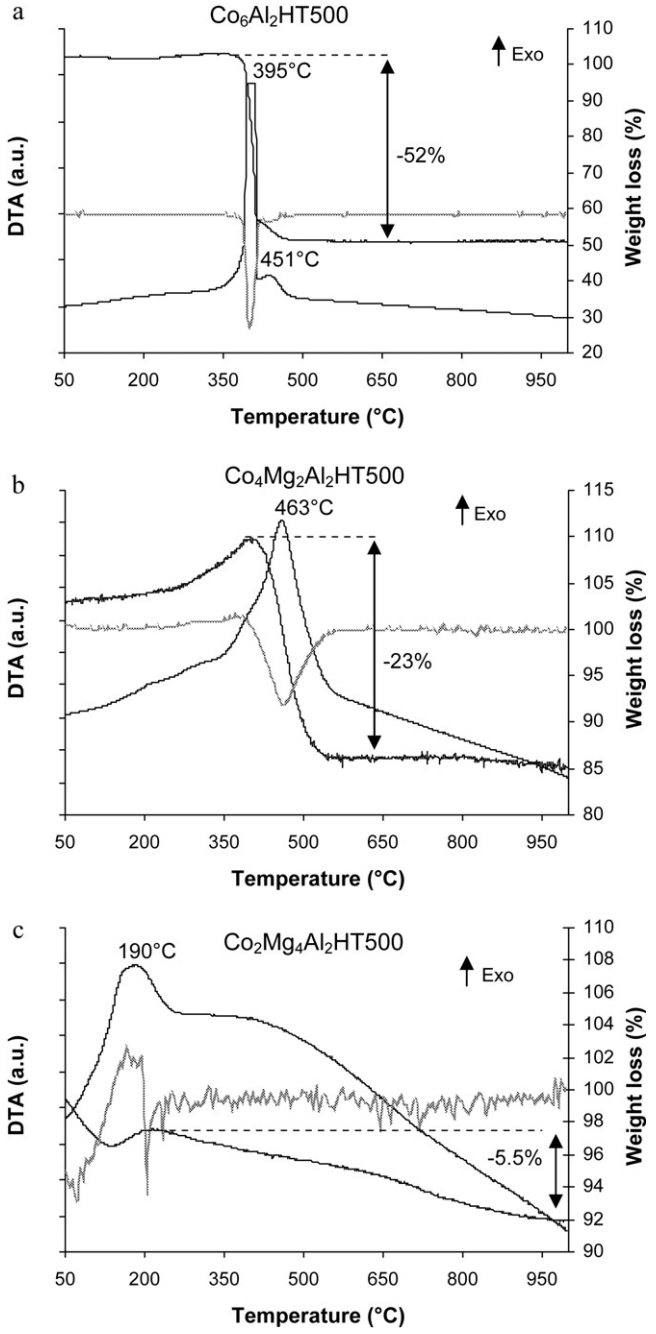

Fig. 5. DTA, TGA and DTG (dotted curves) profiles of Co_6Al_2HT500 reduced sample (a); $Co_4Mg_2Al_2HT500$ reduced sample (b); $Co_2Mg_4Al_2HT500$ reduced sample (c) after stability test.

of $Co_4Mg_2Al_2HT500$ catalyst cannot be the only reason of the deactivation.

Fig. 1b shows the XRD patterns of the catalysts reduced at 800 °C after the CH_4/CO_2 stability reaction. After the reaction the Co^0 phase remained in the catalyst reduced with higher intensities.

The crystallite sizes of the Co^0 before and after test are reported in Table 2. For the $Co_4Mg_2Al_2HT500$ sample, the particle size of Co^0

Table 2
Cristallite size of Co^0 phase before and after test.

Name of samples	Before test (nm)	After test (nm)
Co_6Al_2HT500	–	13
$Co_4Mg_2Al_2HT500$	6	31
$Co_2Mg_4Al_2HT500$	11	16

before (6 nm) and after the test (31 nm) shows a significant sintering phenomenon of Co^0. In this context, the sintering particles are well known to contribute to the deactivation of sample. On the other hand, the smaller particles are known to contribute to the inhibition of the coke deposition. Thus, for the $Co_2Mg_4Al_2$HT500 the stability of crystallite size during the test and the resistance to coking reveals interesting catalytic performances for the CO_2 reforming of methane reaction. Indeed, CO_2 and CH_4 conversions are acceptable with little formation of water and coke. This can be explained by the presence of Co allowing methane and carbon dioxide conversions on one hand and by the considerable amount of magnesium in the sample which makes it possible to attenuate carbon formation on the other hand. $MgAl_2O_4$ oxide detected by XRD in the $Co_2Mg_4Al_2$HT500 sample is known for its basic properties [17]. The presence of this oxide allows CO_2 adsorption on the catalyst and hence, decreases carbon deposit. As suggested in literature [18], carbon deposit can be attenuated or removed if the metal responsible for the catalytic activity is supported on an oxide showing strong basic sites. Mg–Al–O oxide types exhibit various basic functionalities at the surface: weakly basic OH^- groups, medium to medium strong sites connected to the oxygen of Mg^{2+}–O^{2-} pairs and strong basic sites related to isolated O^{2-} anions [17]. The fraction of medium-strong and strong sites increases with the Mg/Al ratio and a high temperature of calcination. Indeed, it has also been assumed that Mg oxides could inhibit coke deposition via adsorbed CO_2 species on the basic site, able to react with the deposited carbon through the reverse Boudouard reaction. Therefore, CO formation by carbon oxidation involves a reduction of the H_2/CO ratio and could explain the reason why this ratio remains lower than 1. $Co_4Mg_2Al_2$HT500, which has a lower Mg content, shows a more important carbon deposit than sample $Co_2Mg_4Al_2$HT500. Thus, for the reaction of dry reforming of methane, catalytic performances of $Co_xMg_yAl_2$HT500 solids depend on Co content in the sample on one hand and on the Mg content on the other hand. These results show that a higher Co content implies higher activity and also higher carbon deposition.

4. Conclusion

The activity and deactivation behaviour of Co–Mg–Al catalyst are studied in carbon dioxide reforming of methane. Catalytic performances of $Co_xMg_{6-x}Al_2$HT500 solids depend on the reduction pretreatment, Co and Mg contents in the sample. Therefore, for $Co_6Al_2Al_2$HT500 higher Co content provides the best activity by the increase of the Co^0 active sites, in contrast it implies a great increase on the amount of coke. The stability of crystallite size of metal particles during the test and the resistance to coking by the presence of $MgAl_2O_4$ phase known for its basic properties mean that the $Co_2Mg_4Al_2$HT500 catalyst is a good compromise between a good activity and a low coke deposition.

References

[1] P. Ferreira-Aparicio, I. Rodriguez-Ramos, J.A. Anderson, A. Guerrero-Ruiz, Appl. Catal. A 202 (2000) 183.
[2] H.Y. Wang, E. Ruckenstein, Appl. Catal. A 209 (2001) 207.
[3] R. Bouarab, O. Akdim, A. Auroux, O. Cherifi, C. Mirodatos, Appl. Catal. A 264 (2004) 161.
[4] A. Djaidja, S. Libs, A. Kiennemann, A. Barama, Catal. Today 113 (2006) 194.
[5] J. Zhang, H. Wang, A. Dalai, Appl. Catal. A 339 (2008) 121.
[6] O.W. Perez-Lopez, A. Senger, N.R. Marcillio, M.A. Lansarin, Appl. Catal. A 303 (2006) 234.
[7] T.-J. Huang, H.-J. Lin, T.-C. Yu, Catal. Lett. 105 (2005) 239.
[8] G. Fornasari, M. Gazzano, D. Matteuzzi, F. Trifiro, A. Vaccari, Appl. Clay Sci. 10 (1995) 69.
[9] C Gennequin, S. Siffert, R. Cousin, A. Aboukais, Top. Catal. 52 (2009) 482.
[10] S. Haag, M. Burgard, B. Ernst, J. Catal. 252 (2007) 190.
[11] C.N. Avila-Neto, S.C. Dantas, F.A. Silva, T.V. Franco, L.L. Romielo, C.E. Hori, A.J. Assis, J. Nat. Gas Sci. Eng. 1 (2009) 205.
[12] J. Guo, H. Lou, H. Zho, D. Chai, X. Zheng, Appl. Catal. A 273 (2004) 75.
[13] S. Takenaka, E. Kato, Y. Tomikubo, K. Otsuka, J. Catal. 219 (2003) 176.
[14] B.S. Liu, C.T. Au, Appl. Catal. A 244 (2003) 181.
[15] S. Wang, G.Q.M. Lu, Appl. Catal. B 16 (1998) 269.
[16] P. Ferreira-Aparicio, C. Marquez-Alvarez, I. Rodrıguez-Ramos, Y. Schuurman, A. Guerrero-Ruiz, C. Mirodatos, J. Catal. 184 (1999) 202.
[17] M.L. Bailly, C. Chizallet, G. Costentin, J.M. Krafft, H. Lauron-Pernot, M. Che, J. Catal. 235 (2005) 414.
[18] K Bachari, R. Bouarab, O. Chérifi, Rev. Energy Renew. 4 (2001) 101.